American Mineralogist, Volume 96, pages 709–715, 2011

Krotite, $CaAl_2O_4$, a new refractory mineral from the NWA 1934 meteorite

Chi Ma,[1,*] Anthony R. Kampf,[2] Harold C. Connolly Jr.,[3,4,5] John R. Beckett,[1] George R. Rossman,[1] Stuart A. Sweeney Smith,[4,6] and Devin L. Schrader[5]

[1]Division of Geological and Planetary Sciences, California Institute of Technology, Pasadena, California 91125, U.S.A.
[2]Mineral Sciences Department, Natural History Museum of Los Angeles County, Los Angeles, California 90007, U.S.A.
[3]Department of Physical Sciences, Kingsborough Community College of CUNY, Brooklyn, New York 11235 and Earth and Environmental Sciences, The Graduate Center of CUNY, New York, New York 10024, U.S.A.
[4]Department of Earth and Planetary Sciences, American Museum of Natural History, New York, New York 10024, U.S.A.
[5]Lunar and Planetary Laboratory, University of Arizona, Tucson, Arizona 85721, U.S.A.
[6]Department of Geology, Carleton College, Northfield, Minnesota 55057, U.S.A.

Abstract

Krotite, $CaAl_2O_4$, occurs as the dominant phase in an unusual Ca-,Al-rich refractory inclusion from the NWA 1934 CV3 carbonaceous chondrite. Krotite occupies the central and mantle portions of the inclusion along with minor perovskite, gehlenite, hercynite, and Cl-bearing mayenite, and trace hexamolybdenum. A layered rim surrounds the krotite-bearing regions, consisting from inside to outside of grossite, mixed hibonite, and spinel, then gehlenite with an outermost layer composed of Al-rich diopside. Krotite was identified by XRD, SEM-EBSD, micro-Raman, and electron microprobe. The mean chemical composition determined by electron microprobe analysis of krotite is (wt%) Al_2O_3 63.50, CaO 35.73, sum 99.23, with an empirical formula calculated on the basis of 4 O atoms of $Ca_{1.02}Al_{1.99}O_4$. Single-crystal XRD reveals that krotite is monoclinic, $P2_1/n$; a = 8.6996(3), b = 8.0994(3), c = 15.217(1) Å, β = 90.188(6), and Z = 12. It has a stuffed tridymite structure, which was refined from single-crystal data to R_1 = 0.0161 for 1014 $F_o > 4\sigma F$ reflections. Krotite is colorless and transparent with a vitreous luster and white streak. Mohs hardness is ~6½. The mineral is brittle, with a conchoidal fracture. The calculated density is 2.94 g/cm^3. Krotite is biaxial (–), α = 1.608(2), β = 1.629(2), γ = 1.635(2) (white light), $2V_{meas}$ = 54.4(5)°, and $2V_{calc}$ = 55.6°. No dispersion was observed. The optical orientation is X = **b**; $Y \approx$ **a**; $Z \approx$ **c**. Pleochroism is colorless to very pale gray, $X > Y = Z$. Krotite is a low-pressure $CaAl_2O_4$ mineral, likely formed by condensation or crystallization from a melt in the solar nebula. This is the first reported occurrence of krotite in nature and it is one of the earliest minerals formed in the solar system.

Keywords: Krotite, $CaAl_2O_4$, new mineral, refractory inclusion, NWA 1934 meteorite, CV3 carbonaceous chondrite, XRD, EBSD

Introduction

A rare $CaAl_2O_4$-dominant Ca-,Al-rich refractory inclusion (CAI), named "Cracked Egg" by Sweeney Smith et al. (2010), is observed in the Northwest Africa (NWA) 1934 meteorite (a CV3 carbonaceous chondrite). During our mineralogy investigation of this CAI, the calcium monoaluminate ($CaAl_2O_4$) was identified as a new mineral, named "krotite." Electron microprobe, high-resolution SEM, electron backscatter diffraction (EBSD), single and powder XRD, and micro-Raman analyses have been used to characterize its composition and structure and the identity and composition of associated phases. Synthetic low-pressure and high-pressure $CaAl_2O_4$ phases are well known in the field of materials science (e.g., Rankin 1915; Hörkner and Müller-Buschbaum 1976; Ito et al. 1980). Dmitryivanovite was recently reported in a CH3 chondrite and described as the high-pressure mineral form of $CaAl_2O_4$ (Mikouchi et al. 2009). Here, we report the first occurrence of the low-pressure polymorph of $CaAl_2O_4$ in nature, as a new refractory mineral, krotite.

Mineral name and type material

The mineral and the mineral name have been approved by the Commission on New Minerals, Nomenclature and Classification (CNMNC) of the International Mineralogical Association (IMA 2010-038). The name is for Alexander N. Krot (born in 1959), a cosmochemist at the University of Hawaii, in recognition of his significant contributions to the understanding of early Solar System processes. Three thin sections (UA2169TS1, UA2169TS2, UA2169TS3) contain the type material. Section UA2169TS1 is deposited under catalog USNM 7590 in the Smithsonian Institution's National Museum of Natural History, Washington, D.C., U.S.A. Co-type material (krotite fragments from Section UA2169TS2) is deposited under catalog 63275 in the Natural History Museum of Los Angeles County, California, U.S.A.

* E-mail: chi@gps.caltech.edu

Occurrence

The NWA 1934 meteorite, which was found at an undisclosed location in north-western Africa, is a CV3 carbonaceous chondrite. The "Cracked Egg" Ca-,Al-rich inclusion (CAI) in this NWA 1934 meteorite is a 2.75 × 4.50 mm object in the section plane sampled by USNM 7590 and surrounded by a matrix of mostly fine-grained olivine. Krotite is the principal phase in the central and mantle regions in Cracked Egg; minor perovskite ($CaTiO_3$), gehlenite ($Ca_2Al_2SiO_7$), hercynite ($FeAl_2O_4$), and Cl-bearing mayenite ($Ca_{12}Al_{14}O_{32}Cl_2$) are present in veins and inclusions in krotite and the entire assemblage is surrounded by a rim (Figs. 1–2). From inside toward the outside, the rim consists of grossite, mixed hibonite and spinel, then gehlenite with an outer layer composed of Al-rich diopside. Trace euhedral hexamolybdenum (Mo,Ru,Pt,Ir,Os) occurs in krotite in the mantle region near the rim and in the grossite layer (Fig. 3). Cracks, which crosscut the rim and portions of the interior, are mainly filled with Fe and Al hydroxides.

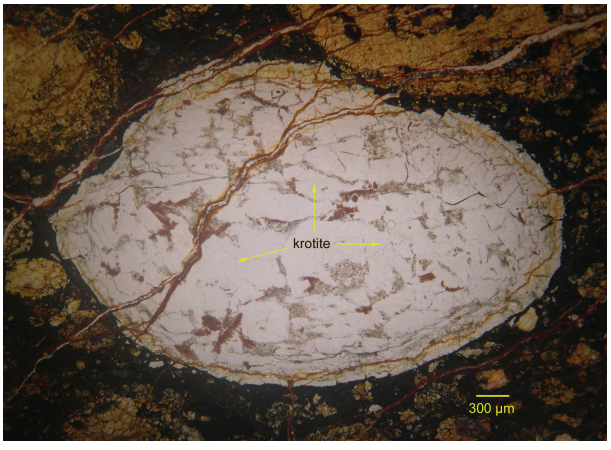

Figure 1. Reflected light photograph of the krotite-dominant CAI in Section UA2169TS2.

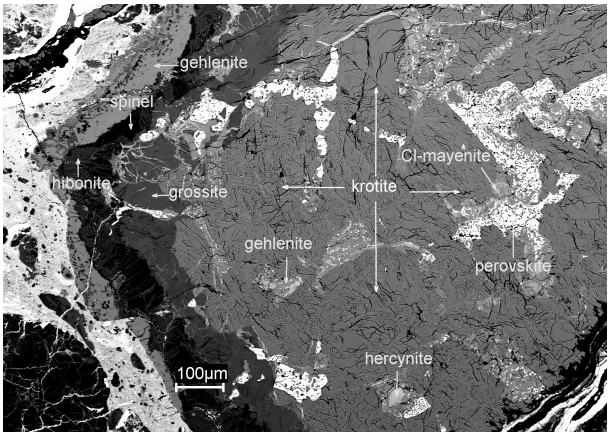

Figure 2. Backscatter electron image showing krotite with perovskite, gehlenite, hercynite, Cl-bearing mayenite, grossite, hibonite, and spinel at one end of the CAI in UA2169TS2.

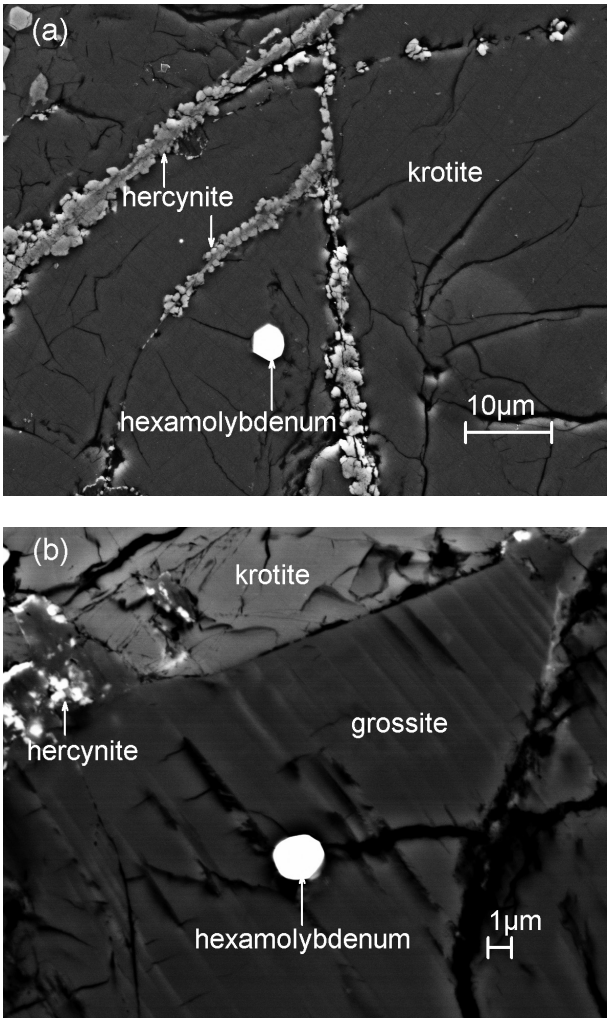

Figure 3. Backscatter electron images showing (**a**) an euhedral hexamolybdenum grain enclosed in krotite near the rim of the CAI in USNM 7590 and (**b**) an euhedral hexamolybdenum grain enclosed in grossite in UA2169TS3.

The Cl-bearing mayenite in Cracked Egg is the first occurrence of this new mineral in a meteorite. The phase is likely formed as an alteration product after krotite in the parent body (Ma et al. 2010).

Hexamolybdenum is a newly discovered Mo-dominant refractory alloy from the Allende CV3 meteorite, where it occurs as inclusions in allendeite, a Sc zirconate and has an empirical formula $Mo_{0.56}Ru_{0.24}Fe_{0.08}Ir_{0.07}Os_{0.03}W_{0.01}Ni_{0.01}$ (Ma et al. 2009). Hexamolybdenum included in krotite and grossite from Cracked Egg is the second natural occurrence. A grain in krotite (Fig. 3a) has a composition $Mo_{0.32}Ru_{0.23}Pt_{0.16}Ir_{0.08}Os_{0.08}V_{0.07}W_{0.02}Rh_{0.02}Ni_{0.01}Fe_{0.01}$. The grain in grossite (Fig. 3b) yields a formula of $Mo_{0.29}Ru_{0.21}Pt_{0.14}Fe_{0.13}Ir_{0.06}Os_{0.06}V_{0.04}Rh_{0.04}Ni_{0.03}W_{0.02}$.

Appearance, physical and optical properties

Krotite occurs as aggregates with the individual crystals ranging from 10 to 350 µm in size, with the largest crystals appearing

near the center of the CAI. Crystals typically exhibit numerous, generally arcuate, fractures and are colorless, transparent, and exhibit a vitreous luster and white streak. Mohs hardness is ~6½. The mineral is brittle, with a conchoidal fracture. Cleavage is good on {100} and {010}. Density could not be measured because of the small amount of material available and its near invisibility in density liquids. The calculated density is 2.944 g/cm^3 for the empirical formula and 2.937 g/cm^3 for the ideal formula. It is non-fluorescent under the electron beam of a scanning electron microscope and under either shortwave (254 nm) or longwave (365 nm) UV radiation. No crystal forms or twinning were observed.

Krotite is biaxial (–), $\alpha = 1.608(2)$, $\beta = 1.629(2)$, $\gamma = 1.635(2)$ (white light), $2V_{meas} = 54.4(5)°$, and $2V_{calc} = 55.6°$. No dispersion was observed. The optical orientation is $X = \mathbf{b}$; $Y \approx \mathbf{a}$; $Z \approx \mathbf{c}$. Pleochroism is colorless to very pale gray, $X > Y = Z$ (barely noticeable). The $2V$ and optical orientation were determined from extinction data using the program EXCALIBRW (Gunter et al. 2004). The Gladstone-Dale compatibility is –0.0186 (superior) based on the empirical formula and –0.0212 (excellent) based on the ideal formula.

Raman spectroscopy

Raman microanalysis of krotite was carried out using a Renishaw M1000 micro-Raman spectrometer system and a 514.5 nm laser calibrated against a silicon standard. A Raman spectrum of krotite was obtained from 4000 to 100 cm^{-1} from a region of the sample free of cracks to minimize contamination from epoxy (Fig. 4). No Raman features were observed between 4000 and 1000 cm^{-1}. In particular, the spectrum gives no indication of either H_2O or CO_2 in the 4000 to 2500 cm^{-1} region. The spectrum was baseline corrected for a weak, broad luminescence band centered near 2400 cm^{-1} that extended across the entire spectrum. The main features are at 141, 150, 174, 312, 404, 456, 520, 543, 647, 686, and 789 cm^{-1}. The most intense bands are at 520 and 543 cm^{-1}. Of all the published synthetic $CaAl_2O_4$ spectra, the krotite spectrum most closely resembles the spectrum of monoclinic $CaAl_2O_4$ (Janáková et al. 2007). Although no complete interpretation of the vibrational spectrum exists, Kojitani et al. (2003) reported a qualitative lattice vibrational calculation for orthorhombic $CaAl_2O_4$ that implies that the bands at less than 250 cm^{-1} are translational modes of Ca^{2+}, bands between 250 and 550 cm^{-1} are rotational modes of AlO_6 polyhedra and translational modes of Al^{3+}. Their calculation further suggests that bands at greater than about 550 cm^{-1} are stretching modes of AlO_6.

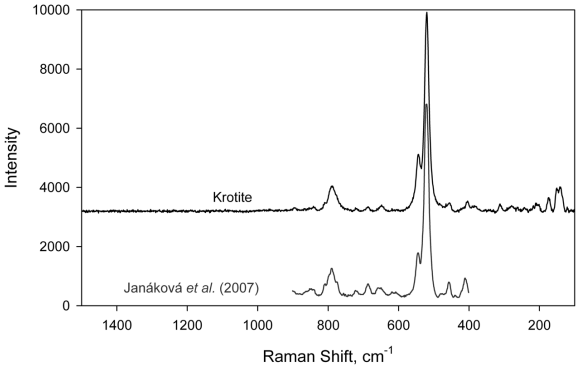

Figure 4. Raman spectra of a single-crystal krotite (this study) and a digitized copy of the spectrum of powdered monoclinic $CaAl_2O_4$ of (Janáková et al. 2007).

Chemical composition

Chemical analyses (7) were carried out using a JEOL 8200 electron microprobe (WDS mode, 15 kV, 25 nA, beam in focused mode). Quantitative elemental microanalyses were processed with the CITZAF correction procedure and the analytical results are given in Table 1. The empirical formula (based on four O atoms) is: $Ca_{1.02}Al_{1.99}O_4$. The simplified formula is $CaAl_2O_4$, which requires CaO 35.48 and Al_2O_3 64.52, total 100.00 wt%.

Crystallography

X-ray diffraction

Both powder and single-crystal X-ray studies were carried out using a Rigaku R-Axis Rapid II curved imaging plate microdiffractometer, with monochromatized Mo$K\alpha$ radiation. For the powder diffraction study, observed *d*-spacings (with standard deviations) and intensities were derived by profile fitting using JADE 9.1 software. The powder data presented in Table 2 show good agreement with the pattern calculated from the structure determination.

The Rigaku Crystal Clear software package was used for reduction of the diffraction data, including the application of an empirical absorption correction. The atomic coordinates of synthetic low-pressure $CaAl_2O_4$ (Kahlenberg 2001) were used as the starting point. Structure refinement, with neutral atom scattering factors, was conducted with SHELXL-97 software (Sheldrick 2008). With anisotropic displacement parameters assigned to all atoms, the final refinement converged to $R_1 = 0.0161$ for 1014 observed reflections with $F_o > 4\sigma F$. Details of the data collection and structure refinement are provided in Table 3. Atomic coordinates and displacement parameters are provided in Table 4, selected bond distances in Table 5, and a bond-valence analysis in Table 6. CIF[1] is on deposit.

Electron-backscatter diffraction (EBSD)

EBSD analyses of krotite single crystals at a submicrometer-scale were carried out with a HKL EBSD system on a ZEISS 1550VP SEM, operated at 20 kV and 6 nA in a focused beam with a 70° tilted stage, using the methods described in Ma and Rossman (2008, 2009). The meteorite sections were final polished with a Buehler VIBROMET2 vibratory polisher using a

[1] Deposit item AM-11-030, CIF. Deposit items are available two ways: For a paper copy contact the Business Office of the Mineralogical Society of America (see inside front cover) for price information. Online, visit the MSA web site at http://www.minsocam.org, go to the *American Mineralogist* Contents, find the table of contents for the specific volume/issue wanted, and then click on the deposit link there.

Table 1. Analytical data for krotite

Constituent*	wt%	Range	St.dev.	Probe standard
Al_2O_3	63.50	63.34–63.67	0.11	spinel
CaO	35.73	35.63–35.83	0.09	anorthite
Total	99.23			

*Si, Mg, Fe, Ti, Na, and K were analyzed but far below detection limit at 99% confidence in weight percent of 0.021, 0.012, 0.029, 0.020, 0.018, and 0.010, respectively.

TABLE 2. X-ray powder-diffraction data for krotite

I_{obs}	d_{obs}	d_{calc}	I_{calc}	*hkl*	I_{obs}	d_{obs}	d_{calc}	I_{calc}	*hkl*	I_{obs}	d_{obs}	d_{calc}	I_{calc}	*hkl*
		5.9280	1	1 1 0			2.2994	1	$\bar{1}$ 3 3			1.6628	1	$\bar{1}$ 3 7
		5.5454	1	0 1 2			2.2976	1	1 3 3			1.6613	1	$\bar{5}$ 1 2
6	5.559(8)	5.5278	2	$\bar{1}$ 1 1			2.2939	2	2 3 0			1.6612	1	1 3 7
		5.5195	2	1 1 1	7	2.278(9)	2.2688	5	$\bar{2}$ 3 1			1.6590	1	3 3 5
28	**4.694(7)**	4.6813	8	$\bar{1}$ 1 2			2.2213	1	$\bar{3}$ 1 4	7	1.6578(16)	1.6556	1	3 3 5
		4.6711	9	1 1 2			2.2017	3	0 3 4			1.6545	1	1 4 5
		4.3882	1	$\bar{1}$ 0 3	11	2.198(3)	2.1973	3	$\bar{2}$ 3 2			1.6542	1	$\bar{2}$ 4 4
15	4.110(9)	4.0497	6	0 2 0			2.1952	3	2 3 2			1.6541	1	4 3 2
		3.9135	1	0 2 1			2.1941	1	$\bar{2}$ 0 6			1.6523	1	4 3 2
		3.8321	1	2 1 0			2.1878	2	2 0 6			1.6501	1	3 4 1
		3.7186	3	$\bar{2}$ 1 1			2.1749	2	4 0 0			1.6441	1	5 0 3
18	3.713(5)	3.7135	7	2 1 1			2.1494	1	0 2 6			1.6077	1	4 3 3
		3.5749	1	0 2 2			2.1402	1	$\bar{3}$ 2 3			1.6053	1	4 3 3
		3.4433	1	0 1 4	12	2.141(4)	2.1359	2	3 2 3			1.5844	1	0 5 2
7	3.420(4)	3.4265	1	$\bar{2}$ 1 2			2.1354	3	$\bar{1}$ 3 4			1.5840	1	$\bar{1}$ 5 1
		3.4185	1	2 1 2			2.1334	1	1 3 4	**23**	**1.5830(20)**	1.5838	1	1 5 1
5	3.312(2)	3.3084	3	$\bar{1}$ 2 2			2.1106	1	$\bar{1}$ 0 7			1.5824	1	0 4 6
		3.3048	2	1 2 2			2.1029	1	$\bar{3}$ 0 5			1.5787	1	$\bar{3}$ 4 3
		3.2049	1	$\bar{1}$ 1 4			2.0960	1	3 0 5			1.5769	1	3 4 3
10	3.205(2)	3.1984	6	1 1 4			2.0929	1	$\bar{4}$ 0 2			1.5765	2	2 3 7
		3.1648	3	0 2 3	7	2.088(6)	2.0893	1	4 0 2			1.5604	2	$\bar{3}$ 3 6
4	3.068(3)	3.0619	4	$\bar{2}$ 1 3			2.0887	1	2 3 3			1.5589	1	$\bar{1}$ 5 2
		2.9760	33	$\bar{1}$ 2 3			2.0799	2	4 1 1			1.5584	1	3 1 8
100	**2.9771(2)**	2.9721	35	1 2 3	13	2.0288(16)	2.0249	7	0 4 0			1.5485	2	$\bar{2}$ 1 9
		2.9640	32	2 2 0			2.0072	1	0 4 1			1.5458	1	4 3 4
		2.9105	4	$\bar{2}$ 2 1			1.9659	1	$\bar{2}$ 3 4			1.5366	3	$\bar{1}$ 2 9
		2.9081	1	2 2 1	5	1.965(6)	1.9629	1	2 3 4			1.5349	5	1 2 9
		2.8756	3	$\bar{1}$ 0 5			1.9601	1	$\bar{3}$ 3 1			1.5314	3	$\bar{1}$ 3 8
		2.8697	1	1 0 5			1.9590	1	3 3 1			1.5309	4	$\bar{4}$ 2 6
		2.8682	1	$\bar{2}$ 0 4			1.9428	2	$\bar{4}$ 1 3	**31**	**1.5279(6)**	1.5267	3	4 2 6
16	2.8630(14)	2.8589	3	2 0 4			1.9291	8	$\bar{2}$ 2 6			1.5260	3	$\bar{5}$ 2 3
		2.8503	4	$\bar{3}$ 0 1	**22**	**1.9267(15)**	1.9249	8	2 2 6			1.5234	4	5 2 3
		2.8489	1	0 1 5			1.9161	8	4 2 0			1.5196	3	$\bar{1}$ 5 3
		2.8469	1	3 0 1			1.8553	1	3 1 6			1.5191	2	1 5 3
		2.7639	1	$\bar{2}$ 2 2			1.8485	1	0 3 6			1.5180	2	2 5 0
		2.7597	1	2 2 2			1.8426	1	$\bar{3}$ 3 3			1.5104	1	2 5 1
		2.6436	1	$\bar{1}$ 2 4			1.8398	1	3 3 3			1.4890	1	$\bar{2}$ 5 2
		2.5785	1	1 3 0	9	1.8409(20)	1.8386	1	$\bar{1}$ 4 3			1.4861	1	2 4 6
		2.5362	18	0 0 6			1.8376	1	1 4 3	2	1.4863(2)	1.4817	1	0 4 7
35	**2.5273(11)**	2.5210	14	$\bar{3}$ 0 3			1.8357	1	2 4 0			1.4816	2	$\bar{4}$ 3 5
		2.5139	14	3 0 3			1.8333	1	$\bar{2}$ 3 5			1.4753	1	$\bar{4}$ 4 1
		2.4413	3	1 3 2			1.8303	1	2 3 5			1.4731	1	1,1,10
		2.4203	9	0 1 6			1.7548	1	$\bar{2}$ 2 7			1.4687	1	1 5 4
40	**2.4101(16)**	2.4071	8	$\bar{3}$ 1 3	4	1.757(4)	1.7514	1	$\bar{1}$ 4 4			1.4627	7	$\bar{3}$ 0 9
		2.4009	10	3 1 3			1.7511	1	2 2 7	**33**	**1.4587(10)**	1.4585	7	3 0 9
		2.3866	3	$\bar{2}$ 1 5			1.7503	1	1 4 4			1.4499	7	6 0 0
		2.3832	1	0 3 3			1.7449	1	$\bar{2}$ 0 8			1.4370	2	$\bar{5}$ 3 2
		2.3446	1	$\bar{1}$ 2 5			1.7254	1	2 4 3			1.4349	1	2,0,10
		2.3406	2	$\bar{2}$ 2 4			1.7027	1	$\bar{2}$ 3 6			1.4341	1	$\bar{4}$ 0 8
		2.3356	1	2 2 4	6	1.691(4)	1.6998	1	2 3 6			1.4234	1	6 0 2
		2.3309	1	$\bar{3}$ 2 1			1.6828	2	4 3 1	6	1.4109(17)	1.4148	1	$\bar{5}$ 1 6
8	2.338(6)	2.3298	4	1 1 6								1.4063	1	$\bar{5}$ 3 3
		2.3290	1	3 2 1										

30 nm non-crystallizing colloidal silica suspension for 2 h to remove deformed surface layers. EBSD analysis was performed in a variable pressure mode (chamber pressure at 25 Pa) on uncoated samples. EBSD patterns of krotite match perfectly with the low-pressure $CaAl_2O_4$ structure (Fig. 5), where indexing is based on a standardized $P2_1/c$ structure transformed from the non-standard $P2_1/n$ structure.

Our initial EBSD analyses led us to incorrectly identify krotite as the high-pressure $CaAl_2O_4$ phase (i.e., dmitryivanovite) because the EBSD program did not correctly load the low-pressure structure from the PDF database due to its non-standard $P2_1/n$ space group. It was only after powder XRD and single-crystal structure analysis that we definitively confirmed it to be the low-pressure phase. Re-examination of our EBSD results revealed that all the patterns were indexed best to the low-pressure structure with a standardized $P2_1/c$ space group transformed from the non-standard $P2_1/n$ space group. We then subsequently compared EBSD patterns for krotite and dmitryivanovite and found that the published EBSD pattern for dmitryivanovite (Mikouchi et al. 2009, Fig. 2) was essentially identical to a pattern we recorded for krotite (Fig. 5c). We note that EBSD analysis can sometimes yield ambiguous structural results and suggest that it would be prudent to confirm the identification of type dmitryivanovite as the high-pressure phase using methods other than EBSD.

Crystal structure

The crystal structure of krotite (Fig. 6) is the same as that of the low-pressure synthetic $CaAl_2O_4$ phase (Hörkner and Müller-Buschbaum 1976; Kahlenberg 2001). It consists of a tetrahedral framework similar to that of tridymite (SiO_2), with Al^{3+} replacing Si^{4+}. Charge balance is maintained by packing Ca^{2+} into the cavities in the framework. Structures such as this are often referred

TABLE 3. Data collection and structure refinement details for krotite

Diffractometer	Rigaku R-Axis Rapid II
X-ray radiation/power	MoKα (λ = 0.71075 Å)/50 kV, 40 mA
Temperature	298(2) K
Structural Formula	$CaAl_2O_4$
Space group	$P2_1/n$
Unit-cell dimensions	a = 8.6996(3) Å
	b = 8.0994(3) Å
	c = 15.2170(11) Å
	β = 90.188(6)°
Z	12
Volume	1072.20(9) Å^3
Density (for above formula)	2.937 g/cm^3
Absorption coefficient	2.102 mm^{-1}
F(000)	936
Crystal size	110 × 60 × 20 µm
θ range	3.44 to 20.81°
Index ranges	$-8 \le h \le 8$, $-8 \le k \le 8$, $-15 \le l \le 15$
Reflections collected/unique	10158/1114 [R_{int} = 0.0264]
Reflections with $F_o > 4\sigma F$	1014
Completeness to θ = 27.48°	99.1%
Max. and min. transmission	0.9592 and 0.8017
Refinement method	Full-matrix least-squares on F^2
Parameters refined	191
GoF	1.116
Final R indices [$F_o > 4\sigma F$]	R_1 = 0.0161, wR_2 = 0.0405
R indices (all data)	R_1 = 0.0192, wR_2 = 0.0416
Largest diff. peak/hole	+0.212/–0.185 e/Å^3

Notes: $R_{int} = \Sigma|F_o^2 - F_o^2(\text{mean})|/\Sigma[F_o^2]$. GoF = $S = \{\Sigma[w(F_o^2 - F_c^2)^2]/(n-p)\}^{1/2}$. $R_1 = \Sigma||F_o| - |F_c||/\Sigma|F_o|$. $wR_2 = \{\Sigma[w(F_o^2 - F_c^2)^2]/\Sigma[w(F_o^2)^2]\}^{1/2}$. $w = 1/[\sigma^2(F_o^2) + (aP)^2 + bP]$ where a is 0.0239, b is 0.5207, and P is $[2F_c^2 + \text{Max}(F_o^2,0)]/3$.

TABLE 5. Selected bond distances (Å) in krotite

Ca1-O3	2.309(2)	Ca2-O10	2.283 (2)	Ca3-O11	2.350(2)
Ca1-O6	2.356(2)	Ca2-O7	2.337(2)	Ca3-O8	2.379(2)
Ca1-O9	2.356(2)	Ca2-O2	2.338(2)	Ca3-O12	2.403(2)
Ca1-O1	2.401(2)	Ca2-O5	2.345(2)	Ca3-O7	2.798(2)
Ca1-O4	2.431(2)	Ca2-O1	2.605(2)	Ca3-O12	2.890(2)
Ca1-O5	2.675(2)	Ca2-O4	2.719(2)	Ca3-O8	2.906(2)
<Ca-O>	2.4213	<Ca-O>	2.4380	Ca3-O11	3.055(2)
				Ca3-O9	3.096(2)
				Ca3-O2	3.183(2)
				<Ca-O>	2.7845
Al1-O8	1.747(2)	Al2-O6	1.757(2)	Al3-O9	1.751(2)
Al1-O3	1.749(2)	Al2-O7	1.757(2)	Al3-O11	1.754(2)
Al1-O4	1.753(2)	Al2-O12	1.758(2)	Al3-O6	1.754 (2)
Al1-O7	1.767(2)	Al2-O4	1.763(2)	Al3-O5	1.769(2)
<Al-O>	1.7539	<Al-O>	1.7587	<Al-O>	1.7570
Al4-O9	1.741(2)	Al5-O2	1.749(2)	Al6-O10	1.750(2)
Al4-O10	1.750(2)	Al5-O3	1.754(2)	Al6-O12	1.752(2)
Al4-O5	1.764(2)	Al5-O11	1.762(2)	Al6-O2	1.757(2)
Al4-O8	1.764(2)	Al5-O1	1.773(2)	Al6-O1	1.763(2)
<Al-O>	1.7546	<Al-O>	1.7593	<Al-O>	1.7554

TABLE 6. Bond-valence analysis for krotite

	Ca1	Ca2	Ca3	Al1	Al2	Al3	Al4	Al5	Al6	Sum
O1	0.309	0.178						0.720	0.739	1.946
O2		0.367	0.037					0.767	0.739	1.910
O3	0.397			0.767				0.758		1.922
O4	0.285	0.131		0.760	0.739					1.915
O5	0.148	0.360				0.727	0.737			1.972
O6	0.349				0.752	0.756				1.857
O7		0.368	0.106	0.731	0.751					1.956
O8			0.328, 0.079	0.771			0.737			1.915
O9	0.349		0.047			0.764	0.785			1.945
O10		0.425					0.766		0.765	1.956
O11			0.355, 0.053			0.757		0.741		1.906
O12			0.308, 0.082		0.749				0.761	1.900
Sum	1.838	1.829	1.396	3.029	2.991	3.004	3.025	2.986	3.004	

Notes: Bond strengths from Brown and Altermatt (1985). Values are expressed in valence units.

to as "stuffed tridymite" structures (Buerger 1954; Glasser and Glasser 1963). In the three-dimensional framework, the tetrahedra form layers consisting of six-membered rings. Different derivatives of the tridymite structure are obtained through variations in the stacking of layers and configurations of the rings. In tridymite, nepheline ($NaAlSiO_4$), and kalsilite ($KAlSiO_4$), there is only one type of ring configuration in which tetrahedra point alternately up (U) and down (D). In krotite and the isostructural minerals beryllonite (Giuseppetti and Tadini 1973), esperite (Tait et al. 2010), and trimerite [$CaMn_2Be_3(SiO_4)_3$] (Klaska and Jarchow 1977), one third of the rings are of the UDUDUD type as in tridymite but two thirds have an UUDDUD configuration. This arrangement leads to two small channel sites in the framework in which large cations are in sixfold coordination and one larger channel site in which the cations are in ninefold coordination. Note that the very low bond-valence sum for the Ca3 site (see Table 6) is typical for this structure type and is indicative of a geometrical mismatch between the Ca^{2+} size and the topology of the UDUDUD rings (Kahlenberg 2001; Tait et al. 2010). At this time, krotite is the only naturally occurring aluminate (i.e., no silicate component) that has a stuffed tridymite structure. In the Strunz System, krotite fits in subdivision 4.BB (oxides with metal:oxygen = 3:4 with only medium-sized cations).

TABLE 4. Atomic coordinates and displacement parameters (Å^2) for krotite

	x	y	z	U_{eq}	U_{11}	U_{22}	U_{33}	U_{23}	U_{13}	U_{12}
Ca1	0.23931(6)	0.03429(7)	0.08926(4)	0.0126(2)	0.0130(4)	0.0129(3)	0.0119(3)	0.0009(3)	0.0022(3)	0.0014(3)
Ca2	0.26876(6)	0.47015(7)	0.07086(4)	0.0138(2)	0.0127(3)	0.0146(3)	0.0141(4)	0.0006(3)	–0.0003(3)	0.0017(3)
Ca3	0.73966(7)	0.52887(7)	0.24701(4)	0.0180(2)	0.0166(4)	0.0176(4)	0.0198(4)	0.0004(3)	–0.0007(3)	–0.0003(3)
Al1	0.42372(9)	0.32738(10)	0.23832(5)	0.0113(2)	0.0110(5)	0.0122(5)	0.0108(5)	–0.0005(4)	0.0010(4)	–0.0001(4)
Al2	0.41960(9)	0.72376(10)	0.23313(5)	0.0112(2)	0.0102(5)	0.0129(5)	0.0105(5)	0.0008(4)	0.0011(4)	0.0000(4)
Al3	0.59857(9)	0.82885(10)	0.07786(5)	0.0112(2)	0.0102(5)	0.0127(5)	0.0107(5)	–0.0002(4)	0.0005(4)	0.0007(4)
Al4	0.61194(9)	0.21941(10)	0.08071(5)	0.0112(2)	0.0107(5)	0.0126(5)	0.0105(5)	–0.0001(4)	0.0007(4)	–0.0005(4)
Al5	0.93519(9)	0.72697(10)	0.09133(5)	0.0111(2)	0.0104(5)	0.0127(5)	0.0101(5)	0.0003(4)	0.0005(4)	–0.0005(4)
Al6	0.93934(9)	0.33446(10)	0.09220(5)	0.0112(2)	0.0103(5)	0.0124(5)	0.0110(5)	0.0002(4)	0.0008(4)	0.0008(4)
O1	0.0764(2)	0.2398(2)	0.02364(12)	0.0146(5)	0.0147(11)	0.0144(11)	0.0147(11)	0.0011(9)	0.0007(9)	0.0004(8)
O2	0.0158(2)	0.5323(2)	0.11035(12)	0.0153(5)	0.0147(11)	0.0146(11)	0.0166(11)	–0.0007(8)	-0.0026(9)	0.0008(9)
O3	0.0541(2)	0.8643(2)	0.14910(12)	0.0151(5)	0.0184(10)	0.0143(11)	0.0127(11)	0.0007(8)	0.0003(8)	–0.0034(9)
O4	0.2478(2)	0.2451(2)	0.20288(12)	0.0148(5)	0.0130(11)	0.0184(11)	0.0131(11)	–0.0034(8)	0.0015(9)	–0.0012(8)
O5	0.4360(2)	0.2590(2)	0.02679(12)	0.0147(5)	0.0131(11)	0.0172(11)	0.0139(11)	–0.0007(9)	0.0003(9)	0.0019(8)
O6	0.4315(2)	0.8532(2)	0.14078(12)	0.0147(5)	0.0129(10)	0.0159(11)	0.0154(11)	0.0031(9)	0.0038(9)	0.0033(9)
O7	0.4344(2)	0.5242(2)	0.18865(12)	0.0162(5)	0.0205(11)	0.0155(11)	0.0126(11)	0.0008(8)	0.0004(9)	–0.0010(9)
O8	0.5843(2)	0.2263(2)	0.19545(12)	0.0152(5)	0.0131(11)	0.0192(11)	0.0132(11)	0.0006(9)	0.0003(9)	0.0037(9)
O9	0.6782(2)	0.0226(2)	0.05493(12)	0.0165(5)	0.0153(10)	0.0163(11)	0.0179(11)	0.0003(9)	0.0043(9)	0.0002(9)
O10	0.7555(2)	0.3562(2)	0.04659(12)	0.0155(5)	0.0147(11)	0.0155(11)	0.0164(11)	0.0023(9)	–0.0009(9)	–0.0004(9)
O11	0.7469(2)	0.7258(2)	0.13366(12)	0.0165(5)	0.0142(11)	0.0209(12)	0.0145(11)	0.0041(9)	0.0012(9)	0.0016(9)
O12	0.9209(2)	0.2454(2)	0.19657(12)	0.0158(5)	0.0126(11)	0.0210(11)	0.0138(11)	0.0013(9)	0.0012(9)	–0.0026(9)

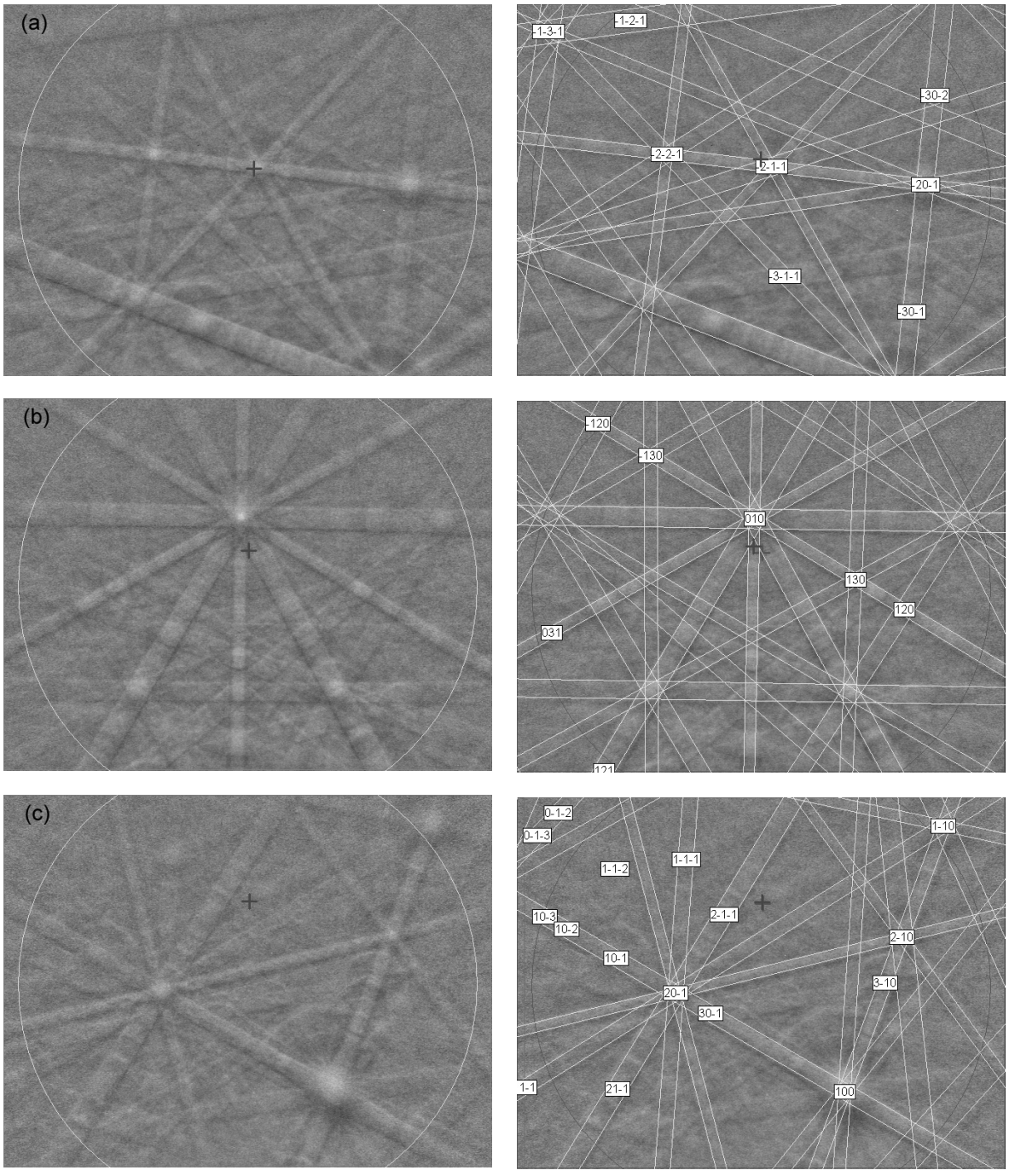

FIGURE 5. EBSD patterns from three krotite grains with different orientations match very well with the low-pressure $CaAl_2O_4$ structure, where indexing is based on a standardized $P2_1/c$ structure transformed from the non-standard $P2_1/n$ structure.

DISCUSSION

A simple model for the formation of "Cracked Egg" is that the inclusion originally consisted mostly of krotite with minor amounts of perovskite, gehlenite, and possibly some additional aluminates. The origin of these "primary" minerals is uncertain but the presence of hexamolybdenum inclusions in krotite and grossite argues for a highly refractory condensate/evaporative environment. This primary phase assemblage was introduced to a hot gas (but not so hot that the inclusion partially melted). The gas, which had a higher partial pressure of Al and lower partial pressure of Ca than needed for equilibrium with krotite reacted with surficial krotite to produce the observed rim sequence krotite

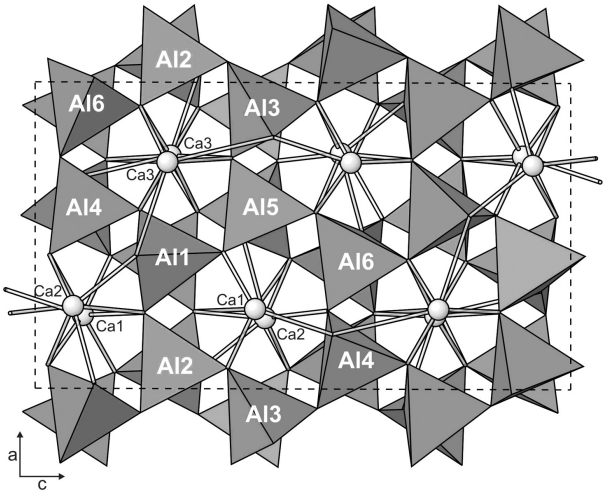

FIGURE 6. Crystal structure of krotite viewed down **b**.

→ grossite → hibonite + spinel → melilite ± spinel. Subsequent to rim formation, a higher temperature event occurred such that the solidus for the interstitial phase assemblage (plus krotite) was exceeded. This melting event led to some corrosion of krotite by the liquid, partial dissolution of perovskite to produce the observed sieve texture and dissolution of some or all of the melilite. Brittle fracture of the rim occurred during or prior to the melting event with some injection of melts into the rim region. Upon cooling, melilite, perovskite, and possibly corundum and mayenite crystallized interstitial to the krotite. Krotite may also have crystallized but, if so, it was in the form of growth on relict krotite as we observe no interstitial krotite crystals. After crystallization, the inclusion would have appeared much as it does now except that corundum and mayenite may have been present and Cl-mayenite and hercynite were absent. A later, lower temperature, stage of alteration/metasomatism introduced Fe and Cl into the interstitial regions leading to the conversion of corundum to hercynite and of mayenite to Cl-mayenite, if they were present. Alternatively, krotite was altered to form Cl-mayenite and hercynite. A final, probably terrestrial, alteration process led to Fe and Al hydroxide filled cracks. Accretion related compaction in the parent body may have caused some of the observed brittle fracture but strong shocks are unlikely to have played a part in the history of this inclusion because the meteorite is essentially unshocked (shock stage S1). A detailed cosmochemical investigation of this krotite-dominant CAI is in progress (Sweeney Smith et al., in prep.).

ACKNOWLEDGMENTS

SEM, EBSD, and electron microprobe analyses were carried out at the Caltech GPS Division Analytical Facility, which is supported, in part, by grant NSF EAR-0318518 and the MRSEC Program of the NSF under DMR-0080065. XRD studies were carried out with support from the John Jago Trelawney Endowment to the Mineral Sciences Department of the Natural History Museum of Los Angeles County. This research was also supported by NSF REU grant no. AST 0851362 and NASA OSS grants no. NNX09AB86G (H.C. Connolly Jr.), and NNX09AG40G (E.M. Stolper). We thank Andrew McDonald, Makoto Kimura, and Takashi Mikouchi for constructive reviews of this manuscript.

REFERENCES CITED

Brown, I.D. and Altermatt, D. (1985) Bond-valence parameters obtained from a systematic analysis of the inorganic crystal structure database. Acta Crystallographica, B, 41, 244–247.

Buerger, M.J. (1954) The stuffed derivatives of the silica structures. American Mineralogist, 39, 600–614.

Giuseppetti, G. and Tadini, C. (1973) Refinement of the crystal structure of beryllonite, $NaBePO_4$. Tschermaks Mineralogishe und Petrographische Mitteilungen, 20, 1–12.

Glasser, F.P. and Glasser, L.S.D. (1963) Crystal chemistry of some AB_2O_4 compounds. Journal of the American Ceramic Society, 46, 377–380.

Gunter, M.E., Bandli, B.R., Bloss, F.D., Evans, S.H., Su, S.-C., and Weaver, R. (2004) Results from a McCrone spindle stage short course, a new version of EXCALIBR, and how to build a spindle stage. Microscope, 52, 23–39.

Hörkner, W. and Müller-Buschbaum, H.K. (1976) Zur Kristallstruktur von $CaAl_2O_4$. Journal of Inorganic and Nuclear Chemistry, 38, 983–984.

Ito, S., Suzuki, K., Inagaki, M., and Naka, S. (1980) High-pressure modifications of $CaAl_2O_4$ and $CaGa_2O_4$. Materials Research Bulletin, 15, 925–932.

Janáková, S., Salavcová, L., Renaudin, G., Filinchuk, Y., Boyer, D., Boutinaud, P. (2007) Preparation and structural investigations of sol–gel derived Eu^{3+}-doped $CaAl_2O_4$. Journal of Physics and Chemistry of Solids, 68, 1147–1151.

Kahlenberg, V. (2001) On the Al/Fe substitution in iron doped monocalcium aluminate – the crystal structure of $CaAl_{1.8}Fe_{0.2}O_4$. European Journal of Mineralogy, 13, 403–410.

Klaska, K.H. and Jarchow, O. (1977) Die Bestimmung der Kristallstruktur von Trimerite $CaMn_2(BeSiO_4)_3$ und das Trimeritgesetz der Verzwillingung. Zeitschrift für Kristallographie und Mineralogie, 145, 46–65.

Kojitani, H., Nishimura, K., Kubo, A., Sakashita, M., Aoki, K., and Akaogi, M. (2003) Raman spectroscopy and heat capacity measurements of calcium ferrite type $MgAl_2O_4$ and $CaAl_2O_4$. Physics and Chemistry of Minerals, 30, 409–415.

Ma, C. and Rossman, G.R. (2008) Barioperovskite, $BaTiO_3$, a new mineral from the Benitoite Mine, California. American Mineralogist, 93, 154–157.

——— (2009) Tistarite, Ti_2O_3, a new refractory mineral from the Allende meteorite. American Mineralogist, 94, 841–844.

Ma, C., Beckett, J.R., and Rossman, G.R. (2009) Allendeite and hexamolybdenum: Two new ultra-refractory minerals in Allende and two missing links. 40th Lunar and Planetary Science Conference, Abstract 1402.

Ma, C., Sweeney Smith, S.A., Connolly, H.C. Jr., Beckett, J.R., Rossman, G.R., and Schrader, D.L. (2010) Discovery of Cl-bearing mayenite, $Ca_{12}Al_{14}O_{32}Cl_2$, a new mineral in a CV3 meteorite. Meteoritics and Planetary Science, 45, Suppl, A123.

Mikouchi, T., Zolensky, M., Ivanova, M., Tachikawa, O., Komatsu, M., Le, L., and Matthieu Gounelle, M. (2009) Dmitryivanovite: A new high-pressure calcium aluminum oxide from the Northwest Africa 470 CH3 chondrite characterized using electron backscatter diffraction analysis. American Mineralogist, 94, 746–750.

Rankin, G.A. (1915) The ternary system CaO-Al_2O_3-SiO_2—with optical study by Fred E Wright. American Journal of Science, 39, 1–79.

Sheldrick, G.M. (2008) A short history of SHELX. Acta Crystallographica, A, 64, 112–122.

Sweeney Smith, S.A., Connolly, H.C. Jr., Ma, C., Rossman, G.R., Beckett, J.R., Ebel, D.S., and Schrader, D.L. (2010) Initial analysis of a refractory inclusion rich in $CaAl_2O_4$ from NWA 1934: Cracked Egg. 41st Lunar and Planetary Science Conference, Abstract 1877.

Tait, K.T., Yang, H., Downs, R.T., Li, C., and Pinch, W.W. (2010) The crystal structure of esperite, with a revised chemical formula, $PbCa_2(ZnSiO_4)_3$, isostructural with beryllonite. American Mineralogist, 95, 699–705.

MANUSCRIPT RECEIVED SEPTEMBER 14, 2010
MANUSCRIPT ACCEPTED JANUARY 29, 2011
MANUSCRIPT HANDLED BY ANDREW MCDONALD